

# Impact of uniformity and biopolymer treatment on base-filter compatibility

**Sungjun Cho, Jongmuk Won**

Department of Civil, Environmental and Architectural Engineering, Korea University, 145, Anam-ro, Seongbuk-gu, Seoul 02841, South Korea, [jmwon@korea.ac.kr](mailto:jmwon@korea.ac.kr)

**Khiem Nguyen Tran Gia**

Department of Civil, Urban, Earth, and Environmental Engineering, Ulsan National Institute of Science and Technology (UNIST), Ulsan, Korea

**ABSTRACT:** Filter design is essential in embankment dams and levees to prevent failures caused by seepage-driven internal erosion. This study presents the impact of uniformity and biopolymer treatment on the base-filter compatibility through soil-column experiments. Five biopolymers (xanthan gum, guar gum, agar gum, chitosan, and zein) and four coefficients of uniformity ( $C_u$ ) were selected to evaluate the optimal biopolymer and the impact of pore size distribution on base-filter compatibility, respectively. The mass of filtrated base sand shown in this study revealed that agar gum was the best-performing biopolymer, with the mitigation of filtrated base sand up to 91% compared to that without biopolymer treatment. In addition, an increase in  $C_u$  a low biopolymer concentration of 0.1% significantly reduced the filtration of base sand. Overall, the results shown in this study show a chance of controlling  $C_u$  or treating with biopolymer to improve the base-filter compatibility by mitigating filtrated base sand.

**KEYWORDS:** base-filter compatibility, biopolymer, coefficient of uniformity, sand, laboratory tests.

## 1 INTRODUCTION

Seepage flow within embankment dams can initiate internal erosion, which may evolve into piping along preferential flow paths, potentially causing failure (Azirou and Benamar, 2013). The piping is frequently observed in dams without filters or with inadequate design of filters. The satisfactory design of the filter materials prevents loss of base soil in embankment with high permeability to dissipate any potential induced pore water pressure. Therefore, filter design is essential to prevent failure of the dam in the event piping initiates (Indraratna et al., 2007).

Previous studies have assessed the occurrence of preventing loss of base soils using filter criteria initially proposed by Terzaghi. Terzaghi's filter criteria rely solely on particle size ratio, proposing effective filters when  $d_{15(filter)}/d_{15(base)} > 4$  and  $d_{15(filter)}/d_{85(base)} < 4$ . Subsequent research has attempted to improve Terzaghi's filter criteria for various types of soils (Bertram, 1940; Sherard & Dunnigan, 1989). Although previous studies continue to improve filter design applicability to a wider range of soils, most of these studies rely on single particle sizes in filter criteria (e.g.,  $d_{15(filter)}$ ,  $d_{15(base)}$ , and  $d_{85(base)}$ ). Bazargan & Eskandari (2013) noted that the coefficient of uniformity ( $C_u = d_{10} / d_{60}$ ) of a filter sand significantly affected the erosion of base sand, indicating the insufficiency of depending on Terzaghi's particle-size criteria in reliably predicting filter performance. Taylor et al. (2019) also found that higher  $C_u$  resulted in smaller pore constrictions, which significantly affect retention and permeability. The abovementioned studies imply that  $C_u$  can be a critical factor affecting base-filter compatibility.

In addition, biopolymers, regarded as environmentally-friendly materials (Fatehi et al., 2024), have been recently studied in soil improvement (Chang & Cho, 2019). The biopolymer-treated soil provides an increase in strength and stiffness of soils (Beguín et al., 2013). In addition, Kwon et al. (2023) provided results of mitigating suffusion through the biopolymer treatment. As inferred from the mitigation of suffusion after biopolymer treatment, the improvement in base-filter compatibility through reduced transport of base-particle into the filter can be anticipated.

Despite the high chance of improving base-filter compatibility by controlling  $C_u$  and biopolymer treatment, the effects of  $C_u$ -controlled and biopolymer-treated sand in filter design remain limited. Therefore, this study comprehensively

investigates the effect of  $C_u$  and biopolymer treatment on contact erosion of fine sand through laboratory soil-column experiments. The mass of filtrated base sand (fine sand) was experimentally evaluated according to the  $C_u$  and biopolymer types. In addition, the treatment efficiency of five biopolymers was quantitatively assessed.

## 2 MATERIALS AND METHODS

### 2.1 Materials

#### 2.1.1 Sand

The types of sand (K1-K8) to control the  $C_u$  of the base (K7) and the filter (K2 or K3) sand, as shown in Figure 1. All properties of the sands used in this study are summarized in Table 1.

Table 1. Properties of sands used in this study.

	K1	K2	K3	K4	K5	K6	K7	K8
$G_s$	2.65	2.65	2.65	2.65	2.65	2.65	2.65	2.65
$e_{max}$	0.96	0.82	0.85	0.97	0.97	1.09	0.97	0.96
$e_{min}$	0.73	0.75	0.73	0.7	0.74	0.79	0.69	0.67
$d_{50}$	4.89	3.16	1.41	2.64	1.62	0.47	0.19	0.12
$d_{85}$	7.27	4.20	2.74	4.12	3.81	0.57	0.27	0.16
$d_{15}$	2.85	2.32	1.06	1.17	0.66	0.35	0.12	0.08
$C_u$	2.17	1.67	1.74	3.21	3.64	1.55	2.03	2.55

Note:  $G_s$  = specific gravity;  $e_{max}$  = maximum void ratio;  $e_{min}$  = minimum void ratio;  $d_{50}$  (mm) = median particle size;  $d_{85}$  and  $d_{15}$  (mm) = diameters corresponding to 85% and 15% finer in the PSD;  $C_u$  = coefficient of uniformity defined as  $d_{60}/d_{10}$ , where  $d_{60}$  and  $d_{10}$  are the diameters corresponding to 60% and 10% finer, respectively, in the PSD;

Figure 2 shows the particle size distributions (PSDs) of the mixed sand corresponding to the  $d_{50}$  of K2, K3, and K7 ( $C_u = 3.67, 5.39,$  and  $7.22$ ), and the original sand of K2, K3, K7, and K8 ( $C_u = 1.67-2.55$ ). The  $d_{50}$  values of the mixed sand was consistent with those of the original K2, K3, and K7 sands. The  $d_{10}$  and  $d_{60}$  values were controlled by combining K1 to K8 sands to control the  $C_u$  of the mixtures. The  $d_{50}$  corresponding to K7 or K8 sands (Figures 2(a) and 2(b)) were selected as base sands, and the  $d_{50}$  corresponding to K2 or K3 sands (Figures 2(c) and 2(d)) were selected as filter sands. The properties of mixed sands used in this study are summarized in Table 2.

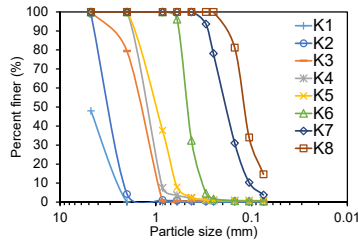


Figure 1. Particle size distributions of K1-K8 sands.

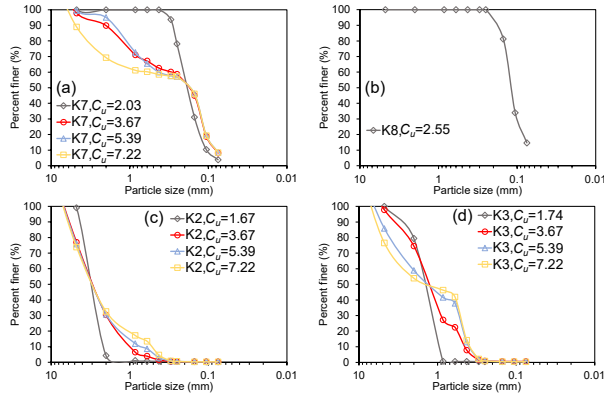


Figure 2. PSD of K7 ((a), K2 ((c)), and K3 ((d)) of original sand ( $C_u = 2.03, 1.67, \text{ and } 1.74$  for K7, K2, and K3, respectively) and mixed sand ( $C_u = 3.67, 5.39, 7.22$ ) and K8 of original sand ((b)) ( $C_u = 2.55$ ).

Table 2. Properties of mixed sands used in this study.

	Mixed sand corresponding to								
	$d_{50}$ of K2			$d_{50}$ of K3			$d_{50}$ of K7		
$C_u$	3.67	5.39	7.22	3.67	5.39	7.22	3.67	5.39	7.22
$G_s$	2.65	2.65	2.65	2.65	2.65	2.65	2.65	2.65	2.65
$e_{max}$	0.76	0.78	0.76	0.81	0.75	0.76	0.73	0.79	0.65
$e_{min}$	0.5	0.51	0.51	0.53	0.48	0.51	0.44	0.51	0.36
$d_{50}$	3.16	3.16	3.16	1.41	1.41	1.41	0.19	0.19	0.19
$d_{85}$	5.4	5.51	5.67	3.24	4.66	5.58	1.7	1.48	4.19
$d_{15}$	1.26	1.04	0.7	0.51	0.44	0.43	0.1	0.09	0.09

### 2.1.2 Biopolymer

Five types of biopolymers (xanthan gum, agar gum, guar gum, chitosan, and zein) were selected to investigate the effect of biopolymer type on the base-filter compatibility and filtration of base sand.

## 2.2 Sample preparation

### 2.2.1 Sample preparation for $C_u$ -controlled test

An acrylic cylindrical column was designed with a total length of 304.8 mm and a diameter of 50.8 mm (Figure 3). As shown in Figure 3, the lower half of the column was filled with K2 or K3 sand (filter sand), and the upper half was filled with K7 or K8 sand (base sand). The perforated metal disks with 2 mm diameter holes were placed at the top and bottom of the column, inducing flow distribution across the cross-sectional area of the column. In addition, a #200 plastic mesh (opening size of 75  $\mu\text{m}$ ) was installed at the bottom of the column to prevent the loss of filter sand during injection. The dampener was placed between the peristaltic pump and the column to inject flow without pulsation. The mass of dry sand corresponding to a relative density of 50% was placed in the acrylic columns using wet pluviation to prepare a saturated sand medium.

Four SRs ( $SR = 8, 12, 17, \text{ and } 27$ ) and four  $C_u$  values ( $C_u = 1.67\text{--}2.55$  (original sand), 3.67, 5.39, and 7.22) were selected as experimental variables. In scenario No. 1, the  $C_u$  of the base sand was kept constant while the  $C_u$  of the filter sand was varied

across experimental conditions. In scenario No. 2, the  $C_u$  of both base and filter sands was varied for experimental conditions. Each case was tested in triplicate to ensure the robustness of experimental results. The average, maximum, and minimum eroded mass of base sand with depth were evaluated.

### 2.2.2 Sample preparation for biopolymer-treated test

The sand was placed in the sonicator bath before being mechanically washed until it reached a turbidity of less than 10 NTU to remove impurities attached to the sand. The washed sand was placed in the column at a relative density of 50%. The K2 sand (filter sand) treated by 0.1, 0.3, 0.5, or 1% of biopolymer solutions was placed in the bottom half of the column, and K8 sand (base sand), which was saturated with deionized water, was placed on top of K2 sand (Figure 3).

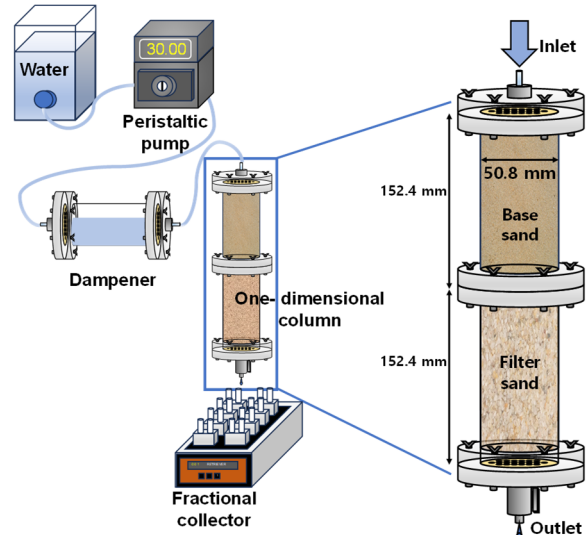


Figure 3. Schematic drawing of the experimental setup and column.

## 2.3 Experimental procedure

In all experiments, deionized water was injected into the column using the peristaltic pump at a flow rate of 30 mL/min (Darcy's velocity = 14.8 mm/min) for 15 pore volumes (PVs). After injection, the remaining deionized water in the acrylic columns was slowly removed to evaluate the mass of filtrated base sand in filter sand. The filter sand was divided into 12 parts to measure the mass of filtrated base sand at every 12.7 mm depth. Furthermore, the fraction of filtrated base sand ( $M_e$ ) was evaluated for quantitative representation of base-filter compatibility in all experimental conditions.

To measure the treatment efficiency of the biopolymer, the biopolymer concentration of samples in the fractional collector (ISCO Retriever II) at the outlet was measured. For the evaluation of biopolymer concentration, turbidity (LUTRON TU-2016) was measured for xanthan gum, guar gum, and agar, whereas the concentration of chitosan and zein was measured by dry weight of samples because of the inability to obtain a linear relationship between turbidity and chitosan or zein concentration.

## 3 RESULTS AND DISCUSSION

### 3.1 Base-filter compatibility

#### 3.1.1 Effect of $C_u$ on base-filter compatibility

Figure 4 presents the mass of filtrated K7 (Figures 4(b), (d), (e), and (f)) and K8 (Figures 4(a) and (c)) sand after injection. Overall, the mass of filtrated base sand decreased with depth, which indicates that no sand was observed at the outlet during

the injection. In addition, the high mass of filtrated base sand at a lower depth of filter sand for all experimental conditions shown in Figure 4 indicates that the filtrated base sand fills the pore of filter sand near the base-filter interface. The filtrated base sand was observed at a depth of  $< \sim 40$  mm for all experimental conditions as shown in Figure 4.

From the observed mass of filtrated base sand shown in Figure 4,  $M_e$  value was calculated as shown in Figure 5. As seen in Figure 5, a decrease in  $M_e$  value with increased  $C_u$  was observed for all experimental conditions. In addition, the reduction of  $M_e$  values become more significant at higher SR at  $C_u = 1.67 - 7.22$  for altering  $C_u$  value of filter sand only (Figures 5(a), 5(b), 5(c), and 5(d)). Furthermore, at given SR, the reduction of  $M_e$  values as  $C_u$  increases becomes more significant for scenario No. 2 than for scenario No. 1. This implies that increase in  $C_u$  of base and filter sand improves base-filter compatibility by reducing pore constriction of the filter sand.

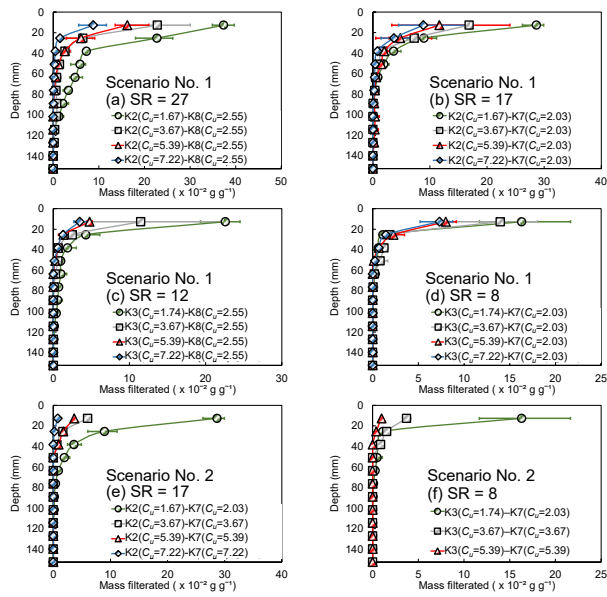


Figure 4. Mass of filtrated base sand for  $C_u$ -controlled experimental conditions.

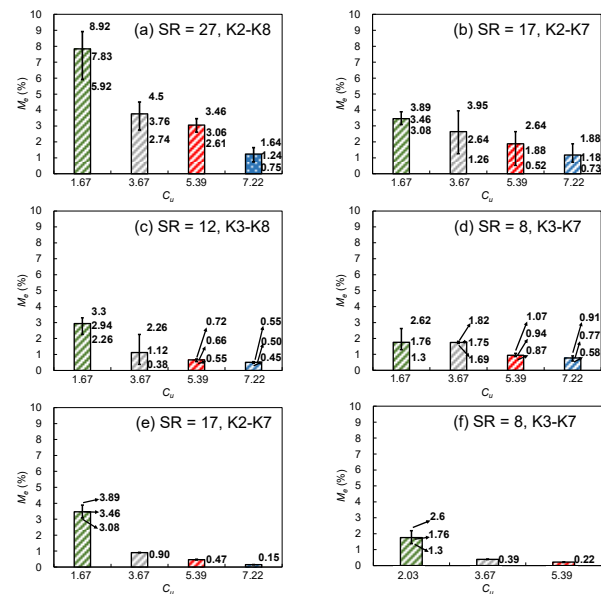


Figure 5. Observed  $M_e$  values for  $C_u$ -controlled experimental conditions.

### 3.1.2 Effect of biopolymer treatment on base-filter compatibility

Figure 6 presents the mass of filtrated K8 sand with depth of K2 sand medium without (Figure 6(a)) and with biopolymer treatment (Figures 6(b)–6(f)). Overall, the mass of filtrated K8 sand decreases as an increase in depth of K2 sand. As seen in Figure 6, a significant reduction of filtrated base sand was observed after biopolymer treatment (Figures 6(b)–6(f)) when compared filtrated mass of base sand for untreated K2 sand (Figure 6(a)). In addition, the depth of filtrated K8 sand was less than 80 mm for all biopolymer-treated sands under all treated concentrations, whereas a higher filtration depth of  $\sim 100$  mm was observed for untreated K2 sand (Figure 6(a)). Therefore, it can be inferred that biopolymer treatment effectively improves the base-filter compatibility.

From the observed mass of the filtrated base sand shown in Figure 6, the  $M_e$  value was calculated and presented in Figure 7. As shown in Figure 7,  $M_e < 3\%$  was obtained for five biopolymer-treated K2 sand regardless of biopolymer concentration, which is even lower than the  $M_e$  value of 7.83% for K2 sand without biopolymer treatment. In addition, relatively similar  $M_e$  values at the four treated concentrations shown in Figures 6 and 7 indicate that the low treated biopolymer concentration of 0.1% can substantially improve the base-filter compatibility.

It is notable that the degree of entanglement among the five biopolymers can be qualitatively assessed from the eroded mass of K8 sand at the interface (Figure 6). From the observed results shown in Figures 6(b)–6(f) for treated concentration of 0.1%, the order of entanglement estimated in this study is chitosan  $\sim$  agar gum  $>$  guar gum  $>$  xanthan gum  $\sim$  zein biopolymer.

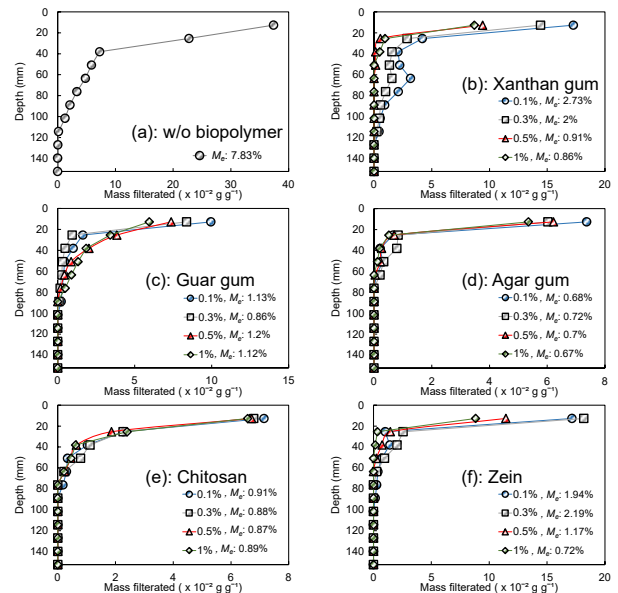


Figure 6. Comparison of mass of filtrated base sand and  $M_e$  values for biopolymer-treated experimental conditions.

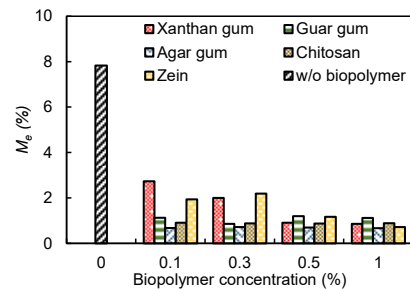


Figure 7. Observed  $M_e$  values for biopolymer-treated experimental conditions.

### 3.2 Efficiency of biopolymer treatment

Figure 8 illustrates the observed normalized biopolymer concentration at the outlet during the injection of deionized water. As seen in Figure 8, normalized biopolymer concentration reached almost zero at  $PV > 2$ . In addition, relatively high mass of biopolymer was observed at the outlet for xanthan gum, guar gum, chitosan, and zein (Figures 8(a), 8(b), 8(d), and 8(e)). In contrast, almost no biopolymer was observed at the outlet for agar gum (Figure 8(c)), implying that the agar gum shows strong binding with sand particles at biopolymer concentrations less than 1%. This can be attributed to the high hydrophilic of agar gum with high solubility and gel-forming property (Chang et al., 2015), which forms a stable and uniform network of agar gum in the pore space of sand medium.

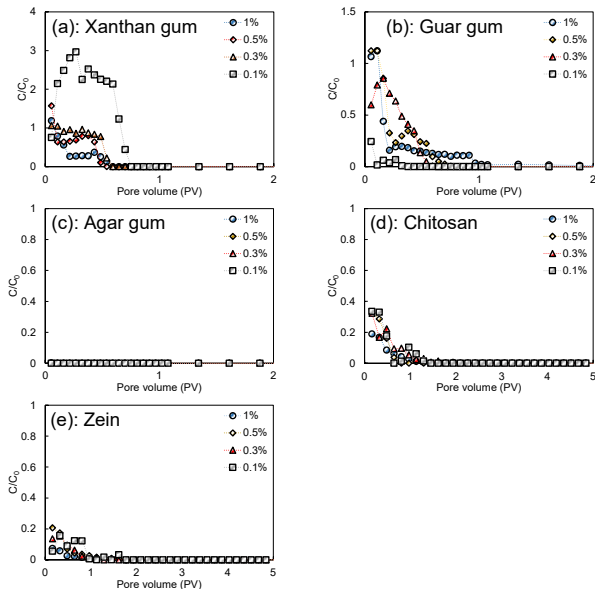


Figure 8. Observed normalized biopolymer concentration ( $C/C_0$ ) of xanthan gum ((a)), guar gum ((b)), agar gum ((c)), chitosan ((d)), and zein ((e)) after deionized water injection.

The area below the breakthrough curve of biopolymer shown in Figure 8 yields treatment efficiency and treated biopolymer mass of five biopolymers as shown in Figures 9(a) and 9(b), respectively. Overall, the treatment efficiency of xanthan gum, chitosan, and zein increases as biopolymer concentration increases, which indicates that an even higher mass of treated biopolymer within the sand matrix can be expected at higher biopolymer concentration in Figure 9(b). In contrast, lower treatment efficiency at higher biopolymer concentration was observed for guar gum (Figure 9(a)). Nevertheless, the higher treated mass of biopolymer was still observed at higher biopolymer concentration (Figure 9(b)). The similar values of  $M_e$  values at biopolymer concentration  $> 0.1\%$  (Figure 7) observed in this study implies that the higher biopolymer concentration for higher treated mass may not be necessary for improving base-filter compatibility.

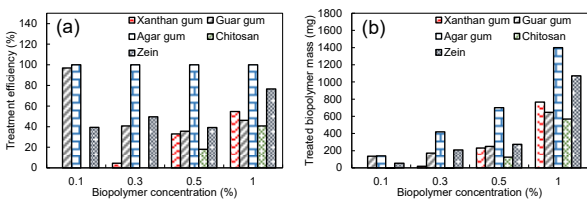


Figure 9. Observed biopolymer treatment efficiency ((a)) and treated biopolymer mass ((b)) in K2 sand medium.

## 4 CONCLUSIONS

This study investigated the impact of coefficient of uniformity ( $C_u$ ) and biopolymer treatment on base-filter compatibility and filtration of base sand. Based on the observed mass of filtrated base sand and biopolymer treatment efficiency the following conclusions can be drawn:

- 1) An increase in  $C_u$  of the filter sand significantly reduced  $M_e$  value, which can also be explained by a lower fraction of pores smaller than filtrated base sand particles at higher  $C_u$  of filter sand.
- 2) The similar  $M_e$  values for treated biopolymer concentrations from 0.1 to 1% shown in this study indicate that 0.1% of biopolymer concentration enables substantial improvement of base-filter compatibility.
- 3) The filtrated mass of K8 sand at the interface between K2 and K8 sand implies that the order of entanglement between biopolymer and sand particles can be estimated as chitosan  $\sim$  agar gum  $>$  guar gum  $>$  xanthan gum  $\sim$  zein.

## 5 ACKNOWLEDGEMENTS

This research was supported by the National Research Foundation of Korea (NRF) Grants funded by the Korean government (No. RS-2022-NR071877 and RS-2026-25467870).

## 6 REFERENCES

- Azirou, S., and Benamar, A. (2013). Assessing the efficiency of filters protecting base soil subject to erosion: No. 1982.
- Bazargan, J., and Eskandari, H.R. (2013). Investigating the Influence of Filter Uniformity Coefficient and Effective Pore Size on Critical Hydraulic Gradient and Maximum Erosion of Dispersive and Non-dispersive Samples: *Journal of Water Sciences Research*, Vol. 5, No. 2, pp. 13–24.
- Beguín, R., Philippe, P., and Faure, Y.-H. (2013). Pore-Scale Flow Measurements at the Interface between a Sandy Layer and a Model Porous Medium: Application to Statistical Modeling of Contact Erosion: *Journal of Hydraulic Engineering*, Vol. 139, No. 1, pp. 1–11, DOI: 10.1061/(asce)hy.1943-7900.0000641.
- Bertram, G.E. (1940). An experimental investigation of protective filters: *Report, Harvard Graduate School of Engineering*, Vol. No. 267(7).
- Chang, I., and Cho, G.C. (2019). Shear strength behavior and parameters of microbial gellan gum-treated soils: from sand to clay: *Acta Geotechnica*, Vol. 14, No. 2, pp. 361–375, DOI: 10.1007/s11440-018-0641-x.
- Chang, I., Prasadhi, A.K., Im, J., and Cho, G.C. (2015). Soil strengthening using thermo-gelation biopolymers: *Construction and Building Materials*, Vol. 77, pp. 430–438, DOI: 10.1016/j.conbuildmat.2014.12.116.
- Fatehi, H., Ong, D.E.L., Yu, J., and Chang, I. (2024). Sustainable soil treatment: Investigating the efficacy of carrageenan biopolymer on the geotechnical properties of soil: *Construction and Building Materials*, Vol. 411, p. 134627.
- Indraratna, B., Raut, A.K., and Khabbaz, H. (2007). Constriction-Based Retention Criterion for Granular filter Design: Vol. 133, No. March, pp. 266–276, DOI: 10.1061/(ASCE)1090-0241(2007)133.
- Kwon, Y.M., Moon, J.H., Cho, G.C., Kim, Y.U., and Chang, I. (2023). Xanthan gum biopolymer-based soil treatment as a construction material to mitigate internal erosion of earthen embankment: A field-scale: *Construction and Building Materials*, Vol. 389, No. January, p. 131716, DOI: 10.1016/j.conbuildmat.2023.131716.
- Sherard, J.L., and Dunnigan, L.P. (1989). CRITICAL FILTERS FOR IMPERVIOUS SOILS: Vol. 115, No. 7, pp. 927–947.
- Taylor, H.F., O'sullivan, C., Shire, T., and Moinet, W.W. (2019). Influence of the coefficient of uniformity on the size and frequency of constrictions in sand filters: *Geotechnique*, Vol. 69, No. 3, pp. 274–282, DOI: 10.1680/jgeot.17.T.051.